

1 **Dissecting the loci underlying maturation timing in Atlantic salmon using haplotype and multi-SNP**
2 **based association methods**

3

4 Marion Sinclair-Waters^{1,2}, Torfinn Nome³, Jing Wang^{3,4}, Sigbjørn Lien³, Matthew P. Kent³, Harald Sægvog⁵,
5 Bjørn Florø-Larsen⁶, Geir H. Bolstad⁷, Craig R. Primmer^{1,2*} & Nicola J. Barson^{3*}

6

7 ¹Organismal and Evolutionary Biology Research Programme, Faculty of Biological and Environmental
8 Sciences University of Helsinki, Helsinki, Finland

9 ²Institute of Biotechnology, Helsinki Institute of Life Sciences, University of Helsinki, Helsinki, Finland

10 ³Centre for Integrative Genetics, Department of Animal and Aquacultural Sciences, Faculty of Biosciences,
11 Norwegian University of Life Sciences, Ås, Norway

12 ⁴Key laboratory for Bio-Resources and Eco-Environment, College of Life Science, Sichuan University,
13 Chengdu, China

14 ⁵Rådgivende Biologer, Bergen, Norway

15 ⁶Norwegian Veterinary Institute, Trondheim, Norway

16 ⁷Norwegian Institute for Nature Research (NINA), Trondheim, Norway

17 *Shared last authors

18

19 **ABSTRACT**

20 Resolving the genetic architecture of fitness-related traits is key to understanding the evolution and
21 maintenance of fitness variation. However, well-characterized genetic architectures of such traits in wild
22 populations remain uncommon. In this study, we used haplotype-based and multi-SNP Bayesian association
23 methods with sequencing data for 313 individuals from wild populations to further characterize known
24 candidate regions for sea age at maturation in Atlantic salmon (*Salmo salar*). We detected an association at
25 five loci (on chromosomes *ssa06*, *ssa09*, *ssa21*, and *ssa25*) out of 116 candidates previously identified in an
26 aquaculture strain with maturation timing in wild Atlantic salmon. We found that at each of these five loci,
27 variation explained by the locus was predominantly driven by a single SNP suggesting the genetic
28 architecture of Atlantic salmon maturation includes multiple loci with simple, non-clustered alleles. This
29 highlights the diversity of genetic architectures that can exist for fitness-related traits. Furthermore, this study
30 provides a useful multi-SNP framework for future work using sequencing data to characterize genetic
31 variation underlying phenotypes in wild populations.

32 INTRODUCTION

33 Understanding the genetic processes underlying fitness variation is a fundamental goal in evolutionary
34 biology. Identifying genetic variants that underlie fitness-related traits is therefore crucial, yet remains
35 challenging. Substantial effort has been made to characterize the genetic architecture of traits – i.e. Are there
36 few or many loci involved? Are loci effects small or large? How are loci distributed across the genome? And
37 what are the allele frequencies at these loci [1–5]? It is generally assumed that in most cases single genetic
38 variants translate into only small changes in complex traits, and therefore follow a polygenic [6,7] or an
39 omnigenic [3,8] model of inheritance.

40 Among genome-wide association studies published to date, many complex traits appear to be
41 polygenic [9]. Although polygenicity is widespread, an increasing number of examples of major effect loci
42 exist, whereby one locus explains a large proportion of the phenotypic variation [10,11]. In some cases,
43 major effect loci can contain multiple tightly linked genes, coined “supergenes”, where localized reduction in
44 recombination is often caused by larger chromosomal rearrangements. For example, this phenomenon is
45 known to underlie phenotypic variation observed among ruff (*Philomachus pugnax*) mating morphs [12,13],
46 Atlantic cod (*Gadus morhua*) [14,15] and rainbow trout (*Oncorhynchus mykiss*) migratory ecotypes [16], and
47 *Heliconius* butterfly wing-pattern morphs [17]. More recent work has found that major effect loci can exist
48 alongside a polygenic background where loci with a variety of effect sizes underlie trait variation [18,19].
49 Such mixed genetic architectures may be pervasive, but currently remain undetected due to the large sample
50 sizes required for detecting loci with smaller effects [19] and it is possible that additional examples are to be
51 found with future higher-powered studies. Although studies aimed at resolving genotype-phenotype links are
52 mounting, well-characterized genetic architectures of fitness-related traits, particularly in natural populations,
53 are still uncommon.

54 While some trait-associated loci have been identified, such findings lead to other crucial questions:
55 How have trait-locus associations arisen? Has the locus arisen through a single or multiple new mutations?
56 Or alternatively, did the locus emerge via recombination that gave rise to new combinations of existing
57 variants? Numerous studies from the past decade have shown that major effect loci involve the cumulative
58 effects of multiple mutations, rather than a single mutation, thus highlighting the relevance of considering the

59 latter scenarios. For example, Bickle et al. [20] found that ~60% of variation in female abdominal
60 pigmentation in *Drosophila melanogaster* can be explained by sequence variation at the *bab* locus, but a
61 GWAS (genome-wide association study) analyzing the same trait did not identify a single SNP in *bab* that
62 passed the genome-wide significance threshold. Alleles consisting of multiple SNPs were associated with
63 high proportions of the variation, whereas, single SNPs had only small effects and were therefore missed in
64 the single-SNP GWAS. Additionally, Linnen et al. [11] and Kerdaffrec et al. [21] also identify multiple
65 mutations within a confined region that have cumulative effects on colour traits in deer mice and seed
66 dormancy in *Arabidopsis thaliana*, respectively. In natural populations with gene flow such as in Linnen et
67 al. [11] and Kerdaffrec et al. [21], this is perhaps not unexpected as theory predicts that clustered and major
68 effect loci will evolve under such scenarios [22,23]. Given these findings, examining extended sequence
69 haplotypes containing multiple SNPs, rather than each SNP independently, is important [24]. This can be
70 achieved by using alternative strategies that look at combined effects of variants, rather than single-SNP
71 methods typically used in GWAS.

72 Here we investigate the genetic basis of Atlantic salmon (*Salmo salar*) sea age at maturity – the
73 number of years spent in the marine environment before reaching maturity and returning to the natal river
74 (freshwater) to reproduce. Age at maturity is an important life history trait affecting fitness traits such as
75 survival, size at maturity and reproductive success [25,26]. Substantial variation in Atlantic salmon sea age
76 at maturity is maintained due to a trade-off between mating success at spawning grounds and survival,
77 whereby individuals that mature later are larger and have higher reproductive success on the spawning
78 grounds, but lower survival and thus lower chance of reaching reproductive age. In contrast individuals that
79 mature early are smaller and have lower reproductive success, but higher survival and thus higher chance of
80 reaching reproductive age [27,28].

81 Variation in maturation timing in Atlantic salmon is highly heritable [19,29,30] and consequently
82 there is substantial interest in understanding the underlying genetic architecture. A large-effect locus on
83 chromosome 25 explaining up to 39% of the variation in sea age at maturity was found in wild European
84 populations [10] and domesticated salmon [31]. The primary candidate gene underlying the association of
85 this locus is *vgll3* due to its close proximity to the associated SNP variation [10,31,32] and its known

86 function in other species. The *vgll3* gene encodes a transcription cofactor that, amongst other things,
87 regulates adipogenesis [33] and is associated with variation in puberty timing in humans [34,35]. In addition
88 to *vgll3*, Sinclair-Waters et al. [19] identified 119 other candidate genes for male maturation in a GWAS
89 including >11,000 males from the same Atlantic salmon aquaculture strain. Two particularly strong
90 associations between maturation timing were found on chromosome 9 in close proximity to *six6* and
91 chromosome 25, *vgll3*. The association of *six6* was also found by Barson et al. [10] in wild Atlantic salmon,
92 however, the signal disappeared after correction for population structure. Interestingly, the *six6* gene is also
93 associated with age at maturity in two Pacific salmon species [36], humans [35] and cattle [37]. However,
94 Barson et al. [10] focused solely on single-SNP associations via GWAS without considering the possible
95 influence of combined variant effects.

96 Studies using sequencing data to examine variation associated with important fitness-related traits in
97 wild populations are limited. However due to developments in sequencing technologies and bioinformatics,
98 studies using this approach are likely to rise in number. We therefore aim to provide a useful and timely
99 framework for characterizing genetic variation underlying phenotypes in wild populations in the future.
100 Here, we focus on further characterizing the association between the loci identified in Sinclair-Waters et al.
101 [15] and sea age at maturity in wild Atlantic salmon. We integrate re-sequencing data and phenotype
102 information for 313 individuals from 53 wild population of Atlantic salmon with alternative GWAS
103 strategies that consider the combined effects of variants, rather than single-SNP effects. This approach can
104 provide better resolution of the variants that are potentially involved in controlling fitness-related traits such
105 as maturation timing in Atlantic salmon.

106

107 METHODS

108 *Study material*

109 Whole genome sequencing data was obtained for 313 wild individuals collected from 53 Norwegian
110 and Finnish populations spanning the Norwegian coast and to the Barents sea in the north (59°N - 71°N)
111 (Supplementary Table S1) previously reported in Bertolotti et al. [38]. The 313-individual dataset includes

112 populations belonging to both the Atlantic and Barents/White sea phylogeographic groups. These regions
113 were studied in Barson et al. [10] using SNP-array data and a single SNP approach, therefore missing
114 variants and potentially combined variant effects. Individuals were categorized into three maturation
115 categories based on the number of years spent at sea prior to their first return migration to rivers for
116 spawning: 1 (one year spent at sea), 2 (two years spent at sea), or 3 (three or more years spent at sea). Only
117 five individuals had spent four years and were therefore combined with three-year fish for all analyses.

118 *SNP calling & filtering*

119 Variant calling and the first round of filtering was done in a larger set of individuals described in
120 Bertolotti et al. [38]. Raw Illumina reads were mapped to the Atlantic salmon genome (ICSASG_v2) [39]
121 using *bcio-nextgen v.1.1* [40] with the *bwa-mem aligner v.0.7.17* [41]. Genomic variation was identified
122 using the Genome Analysis Toolkit (*GATK v4.0.3.0.*), following *GATK*'s best practice recommendations.
123 *Picard v2.18.7* [42] was used to mark duplicates and *GATK* was used for joint calling [43]. Variants were
124 annotated using *SNPeff v. 4.3* [44]. Variant call were further filtered with *GATK*'s variant filtration
125 according to the following *--filterExpression*: "MQRankSum < -12.5 || ReadPosRankSum < -8.0 || QD < 2.0
126 || FS > 60.0 || (QD < 10.0 && AD[0:1] / (AD[0:1] + AD[0:0]) < 0.25 && ReadPosRankSum < 0.0) || MQ <
127 30.0". SNPs were then filtered using *SNPable* procedure [45], where 100 bp kmers are mapped to reference
128 genome (ICSASG_v2) using Burrows-Wheeler Aligner (*bwa aln*) [46], and only SNPs within regions with
129 reads that uniquely map are retained. We then removed additional SNPs with *vcftools* using the following
130 criteria: *--min-alleles 2*, *--max-alleles 2*, *--maf 0.000000001*, *--max-missing 0.7*, *--remove-indels*, *--minGQ*
131 *10*, and *--minDP 4*. A subset 313 individuals from wild populations was then extracted from this larger
132 dataset using *vcftools* [47]. This reduced dataset was used for all subsequent analyses.

133 *Principal component analysis*

134 We produced a reduced SNP dataset by pruning one SNP from each SNP pair with a correlation
135 coefficient (r^2) greater than 0.2 within a 50 kb block using the *--indep-pairwise 50 10 0.2* function
136 implemented in *PLINK v1.9* [48]. This yielded 403,540 SNPs to examine population structure using a
137 principal component analysis, *smartpca*, implemented in the EIGENSOFT v5 software [49].

138 *Data preparation*

139 In this study, we focus on genomic regions containing the 116 candidate loci for age at maturity
140 identified in Sinclair-Waters et al. [19]. We extracted SNP genotype data from 500 kb regions surrounding
141 the 116 trait-associated SNPs identified in Sinclair-Waters et al. [19] using *vcftools*' [47] position filtering
142 functions *--from-bp* and *--to-bp*, as well as allele filtering function *--mac 1* to keep only polymorphic sites.
143 SNPs that were within 250 kb of an adjacent SNP were analyzed together by examining a region that extends
144 250 kb upstream of the first SNP to 250 kb downstream of the last SNP.

145 The current Atlantic salmon genome (ICSASG_v2) contains a known assembly error within the 500
146 kb region surrounding the known candidate loci *vgll3* [31]. A misplaced and misoriented scaffold currently
147 placed downstream of *vgll3* belongs within a gap in the assembly just upstream of *vgll3* on ssa25. For this
148 reason, we constructed a revised assembly for this chromosome. SNP calling was performed as described
149 above. We then retained SNPs that had met the filtering criteria. A total of 8 candidate SNPs are located
150 within regions of the genome that were moved. To find the position of these SNPs in the revised
151 chromosome 25 sequence, we extracted 200 bp surrounding each of these SNPs from the current genome
152 assembly (ICSASG_v2) using the *getfasta* function in *BEDTools* [50]. The 200 bp sequence was then blasted
153 to the fixed assembly to determine the new position of each SNP using Blast's *blastn* function [51]. Using
154 the new SNP positions, SNP genotypes within a 500 kb region surrounding the moved candidate SNPs were
155 extracted from the fixed dataset using *vcftools*.

156 *Association testing at candidate regions*

157 We applied three association mapping methods to describe the genetic architecture underlying sea age
158 at maturity at each of the candidate regions identified in Sinclair-Waters et al. [19]. First, a multi-SNP
159 approach examining associations between phenotype and haplotypes was conducted using Bayesian linear
160 regression implemented in *hapQTLv1.00* [52]. In this approach, a hidden Markov model is used to
161 characterize haplotype structure and ancestry [53]. Haplotype sharing at each marker is then used to quantify
162 genetic similarity among individuals. Haplotype associations are identified by testing for an association
163 between genetic similarity at each marker and the phenotype [52]. Each of the extracted *vcf* files was

164 converted to *bimbam* format using *PLINK 1.9* [54]. The resulting *bimbam* files were used as input for
165 *hapQTL*. Second, single SNP associations were also identified using a Bayesian linear regression method
166 implemented in *hapQTL* [55]. For all *hapQTL* association tests, sex and the six most significant principal
167 components (see above) were included as covariates in the models. Each *hapQTL* run consisted of 2 EM runs
168 (-e 2) with 40 steps (-w 40), 2 upper clusters (-C 2), 10 lower clusters (-c 10). Three replicate *hapQTL* runs
169 were performed for each of the 116 selected regions. Based on recommendations from Jeffreys [56], Bayes
170 factors greater than three were considered evidence for an association of either SNPs or haplotype with sea
171 age at maturity phenotype.

172 Third, a multi-SNP approach aimed to estimate the number and identity of SNPs underlying trait
173 variation at each candidate region using Bayesian Variable Selection regression implemented in *PiMASS*
174 [55]. Due to computational restrictions, the *PiMASS* analysis was performed for only candidate regions that
175 had a SNP or haplotype association with Bayes factor greater than 3. Prior to the *PiMASS* analysis, all
176 missing genotypes were imputed in *BIMBAM* [55] as mean genotypes (-wmg) using default settings.
177 Additionally, our phenotype values for sea age at maturity were adjusted to correct for confounding effects
178 of sex and population structure by regressing the phenotype on sex and the six most significant principal
179 components (see above) using the *lm* function in *R*. *PiMASS* was run with the residual phenotype values. We
180 placed priors on the proportion of variance explained by SNP(s) ($h_{\min} = 0.001$ and $h_{\max} = 0.999$) and the
181 number of SNPs in the model ($p_{\min} = \log \frac{1}{N}$ and $p_{\max} = \log \frac{300}{N}$, where N is the total number of SNPs). Each
182 run consisted of a burn-in of 1000000 steps, followed by 2500000 steps where parameter values were
183 recorded every 1000 steps. For each analysis, we examined the posterior inclusion probability for each SNP,
184 the distribution of the number of included SNPs and the distribution of the proportions of variance explained
185 per model. We also examined the path of estimated Bayes factors and parameter values (h , p , s) across all
186 recorded iterations to check for convergence of runs.

187 To further assess whether more than one SNP in a candidate region was significantly associated with
188 sea age at maturity, we regressed out the top-associated SNP from the residual phenotype values described
189 above and reran *PiMASS* using the previously-used priors and settings. We then examined the posterior
190 inclusion probability for each SNP, the distribution of the number of included SNPs, and the distribution of

191 proportion of variance explained to determine whether there was evidence for multiple SNP associations
192 within a given candidate region.

193

194 RESULTS

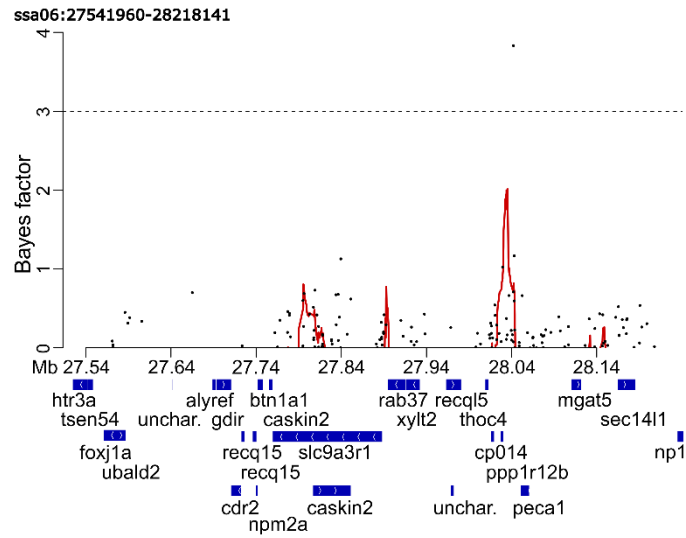
195 *Principal component analysis*

196 The first six principal components (PCs) calculated with the pruned SNP dataset explained 1.96%,
197 0.68%, 0.63%, 0.59%, 0.56% and 0.51% of the genetic variance, respectively (Supplementary Figure S1).
198 These six PCs were included in subsequent association analyses to reflect population structure among
199 samples.

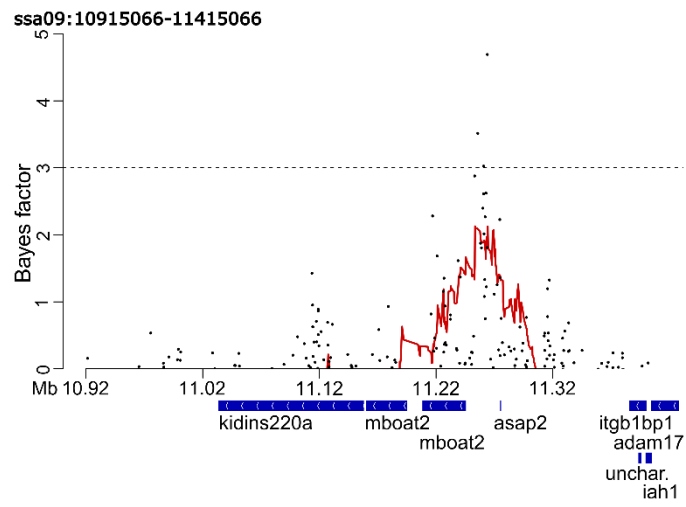
200 *Associations identified with hapQTL*

201 Single-SNP and haplotype association analyses with *hapQTL* revealed strong (Bayes factor > 3)
202 association signals at 5 of the 116 candidate regions (Figure 1, Supplementary Figure S2). The strongest
203 association observed within each region was with a single SNP, rather than an extended haplotype,
204 suggesting a single mutation underlies the effect of each of these regions on maturation timing. However,
205 exceptions occurred in the ssa09:24636574-25136574 and ssa25:28389273-28889273 regions, where second
206 association signals were found upstream of the primary association signal and were most strongly linked to
207 an extended haplotype. For instance, strong haplotype association scores (Bayes factor > 3) spanned a 26971
208 bp region (ssa09:24781742-24808713) containing an uncharacterized gene (LOC106610978) and *pcnx4*. In
209 the ssa25:28389273-28889273 region, a strong haplotype signal was found within *edar* (Figure 1).

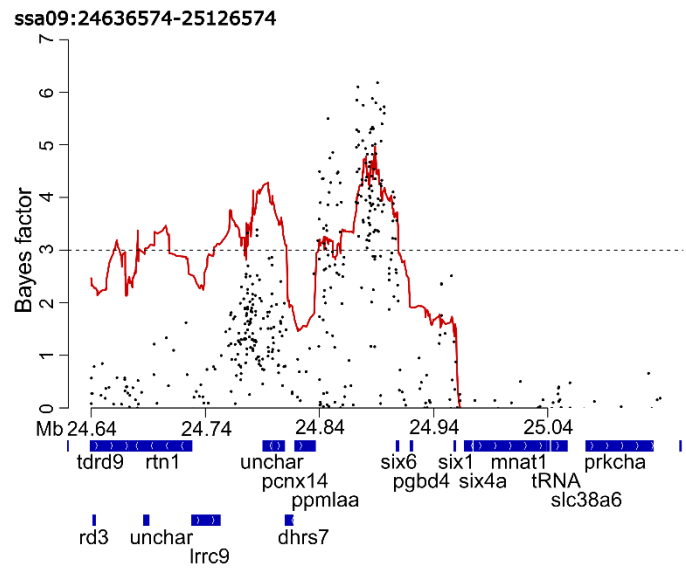
210 We find differences in the location of the top-associated SNPs found here and those identified in
211 Sinclair-Waters et al. [19]. For regions ssa06:27541960-28218141, ssa09:10915066-11415066 and
212 ssa25:28389273-28889273, the top-associated SNP was located further upstream than in Sinclair-Waters et
213 al. [19]. Contrastingly, the strongest associated SNPs within the regions ssa09:24636574-25136574 and
214 ssa21:49390687-49890687 differed only slightly (<5000 bp) between studies (Table 1).



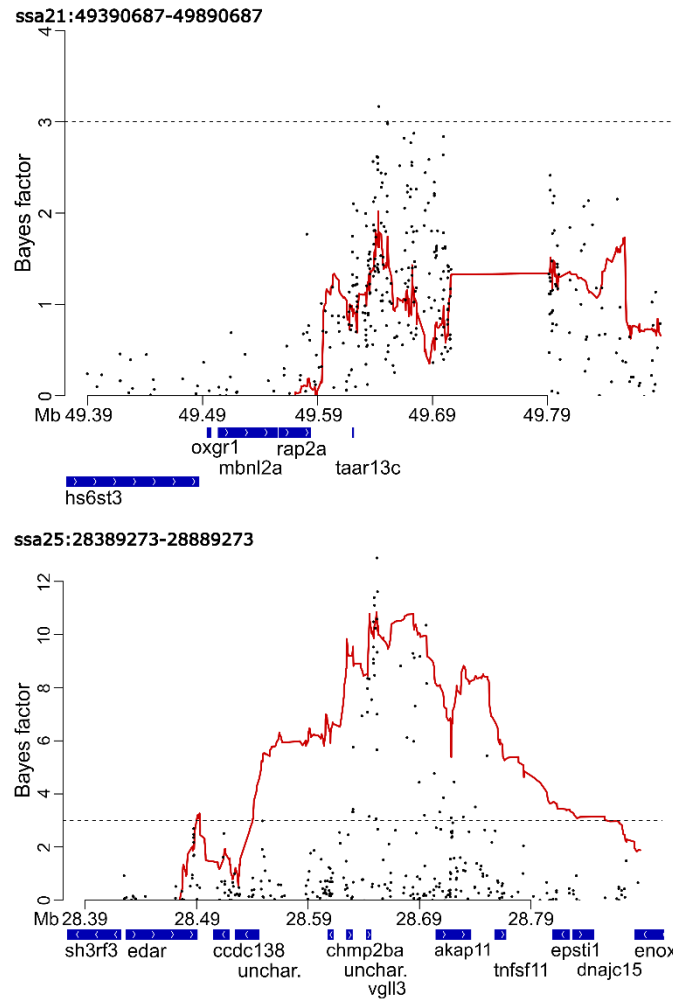
215



216



217



218

219

220 Figure 1. Plots displaying single SNP associations (black points) and haplotype associations (red line) scores
221 from *hapQTL* for the five candidate regions with Bayes factors greater than 3. Y-axis shows the Bayes factor
222 indicating the association strength. X-axis shows the position on the respective chromosomes.

223 Table 1. Strongest association signals for each candidate region showing evidence of an association with sea age at maturity, the genes in closest proximity
 224 and association values from *hapQTL*. Top SNPs for each region from previous SNP-array study [19].

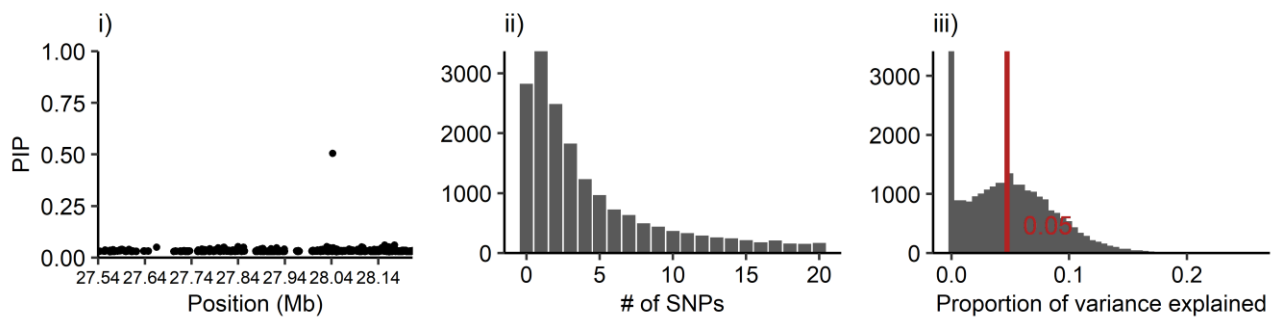
Candidate region	Top signal	Closest gene	Bayes Factor	$-\log_{10}(P\text{-value})$	Allele frequency	Top SNP(s)^a	Candidate gene(s)^a
ssa06:27541960-28218141	6:28045390 (SNP)	<i>pecam1</i> (intron)	3.835	5.107	0.320	6:27791960 6:27968141	<i>slc9a3r1</i> <i>recql5</i> LOC106606978
ssa09:10915066-11415066	9:11266848 (SNP)	<i>asap2a</i> (upstream)	4.696	5.434	0.074	9:11165066	<i>mboat2</i>
ssa09:24636574-25136574	9:24888841 (SNP)	<i>six6</i> (upstream)	6.184	4.242	0.425	9:24886574	<i>six6</i>
ssa21:49390687-49890687	21:49645222 (SNP)	<i>taar13c</i> (upstream)	3.172	4.649	0.464	21:49640687	<i>taar13c</i>
ssa25:28389273-28889273	25: 28651640 (SNP) [ICSASG_v2: 25:28669350]	<i>vgll3</i> (downstream)	12.893	6.406	0.358	25:28910202	<i>vgll3</i>

225 ^aFrom Sinclair-Waters et al. [19].

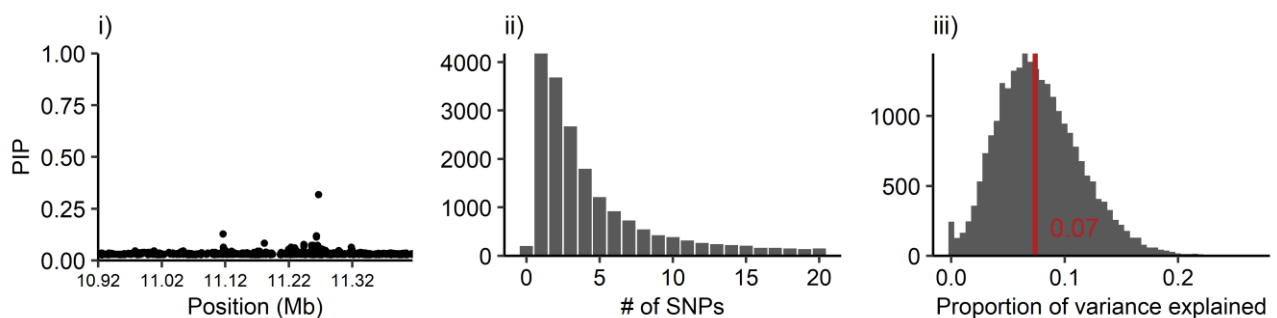
226 *Multi-SNP associations identified using PiMASS*

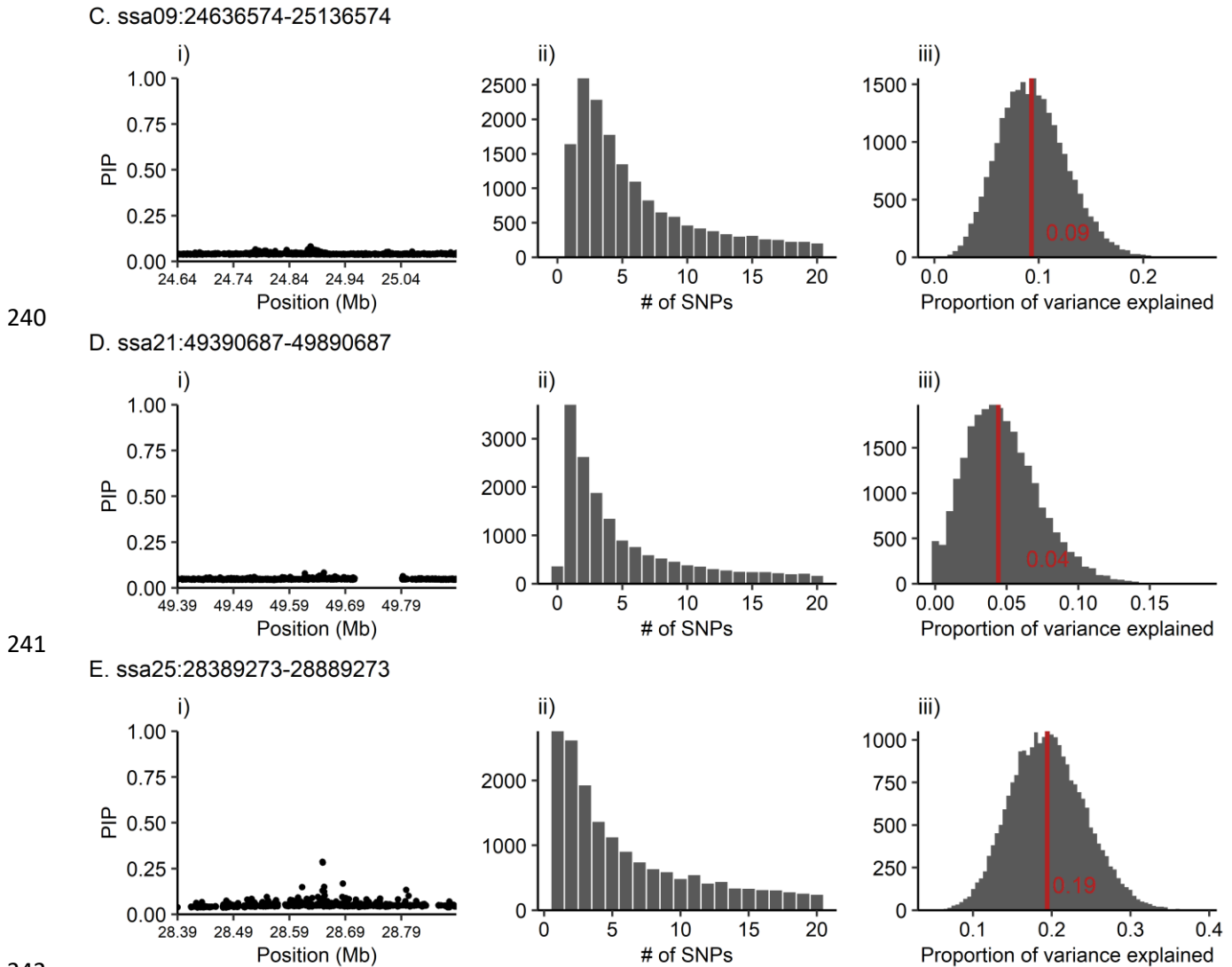
227 Multi-SNP association analysis with *PiMASS* showed that at four of five candidate regions, a single-
228 SNP model was most commonly used to explain variation in sea age at maturity. At one candidate region,
229 ssa09:24636574-25136574, a multi-SNP model including two SNPs was most commonly used to explain
230 variation in sea age at maturity. Median proportion of variance explained by each candidate region ranged
231 between 4% and 19% (Figure 2, Table 2). However, when the top-associated SNP was regressed out from
232 the phenotype values, no SNPs were selected to explain sea age at maturity for all five candidate regions.
233 Additionally, post-regression median proportion of variance was substantially lower – ranging between 0%
234 and 1% (Supplementary Figure S3, Table 2). This would suggest that sea age variation explained by each of
235 these regions is largely driven by a single mutation. We observe no obvious trends in parameter values or
236 Bayes factors, suggesting models converged and burn-in period was adequate (Supplementary Figure S4
237 &S5).

A. ssa06:27541960-28218141



B. ssa09:10915066-11415066





243 Figure 2. *Pi*MASS results for each of the tested candidate regions: A. ssa06:27541960-28218141, B.
244 ssa09:10915066-11415066 C. ssa09:24636574-25136574, D. ssa21:49390687-49890687, and E.
245 ssa25:28389273-28889273. Plots display the following results for each candidate region: i) posterior
246 inclusion probability (PIP) indicating the probability of a SNP being included in a model explaining sea age
247 at maturity variation, ii) truncated distribution of the number of SNPs included in a model explaining sea age
248 at maturity variation, and iii) distribution of proportion of variance explained per recorded iteration (2500).
249 Red line indicates the median proportion of variance explained.

250

251 Table 2. *PiMASS* results prior to and after regression of top-associated SNP identified in the initial *PiMASS*
 252 analysis. These include the mode of the distribution of the number of SNPs and the median of the
 253 distribution of proportion of variance explained (PVE) for a model explaining sea age at maturity.

Candidate region	Mode # of SNPs	Median PVE	Mode # of SNPs (post-regression)	Median PVE (post-regression)
ssa06:27541960- 28218141	1	0.05	0	0
ssa09:10915066- 11415066	1	0.07	0	0.01
ssa09:24636574- 25136574	2	0.09	0	0.01
ssa21:49390687- 49890687	1	0.04	0	0
ssa25:28389273- 28889273	1	0.19	0	0.01

254

255

256 DISCUSSION

257 Despite that combined effects of multiple variants at trait-associated loci are playing an important role
 258 in controlling fitness traits across a variety of species [11,20,21], our results indicate that sea age at
 259 maturation in Atlantic salmon is predominantly associated with single SNP variation at candidate regions.
 260 Using resequencing data to analyse 116 candidate loci and an analytical framework aimed at detecting multi-
 261 SNP associations, we find that single SNPs explain the variation in sea age at maturity in almost all cases.
 262 This work targeting candidate genes identified in aquaculture salmon strains suggests a mixed genetic
 263 architecture where a combination large-effect loci and smaller-effect loci also underlies age at maturity in
 264 wild Atlantic salmon populations. Two core loci, *vgl13* and *six6*, likely play a key role in determining age at
 265 maturity and additional smaller effect loci may be important for fine-tuning the trait across heterogeneous
 266 environments.

267 Theoretical modelling predicts that clustering of tightly linked adaptive mutations will occur under
 268 gene flow and selection in populations inhabiting spatially and/or temporally heterogeneous environments
 269 [22,23]. Although this seems to be a plausible scenario under which the genetic architecture of age at
 270 maturity has evolved in Atlantic salmon, our work suggests that the association in each of the candidate
 271 regions is driven by a single mutation. We cannot rule out, however, the possibility that the examined
 272 regions have pleiotropic effects and contain SNPs controlling other adaptive traits that have weak or no
 273 correlation with maturation timing. It is also possible that we did not have sufficient power to detect

274 additional SNPs in these regions with small effects or with rare alleles. However, previous empirical studies
275 have found few, but complex, loci with clusters of adaptive mutations [11,20,21], thus motivating our
276 investigation of multi-SNP and haplotypic effects. Remington [24] also highlights the importance of
277 distinguishing between allelic effects and single mutational effects when examining the genetic architecture
278 of adaptive variation and its evolution. Our findings, however, suggest that alternative genetic architectures
279 are feasible. One possible explanation could relate to the multiple whole genome duplication events that have
280 occurred in Atlantic salmon and other salmonids [57]. The presence of multiple gene copies may impact the
281 evolution of genetic architecture for traits such as age at maturity in Atlantic salmon. It is also possible that
282 gene flow among Atlantic salmon populations is too restricted to neighbouring populations and/or strength of
283 selection is insufficient for the establishment of linked mutations, as there is a rather specific balance of gene
284 flow and selection required for clustered loci to arise [58]. Both an extension of models predicting genetic
285 architecture and additional empirical studies – on a wider variety organisms and traits – are needed to
286 evaluate the generality of particular architectures and to further understand the conditions under which they
287 evolve.

288 We find additional evidence that a large-effect locus on *ssa25*, *vgll3*, largely underlies age at maturity
289 in Atlantic salmon corroborating findings from a number of association studies on Atlantic salmon
290 maturation [10,19,31,32,59]. The second strongest associated locus in this study is located in close proximity
291 to *six6* on *ssa09*. This locus was previously found to be associated with early maturation in male farmed
292 Atlantic salmon [19], with sea age at maturity in wild Atlantic salmon prior to population structure correction
293 [10] and two species of Pacific salmon (Sockeye salmon and Steelhead trout) [36]. Additionally, we found
294 another three loci associated with sea age at maturity: *pecam1*, *asap2aa* and *taar13c*. The handful of loci
295 found here suggests that wild Atlantic salmon have a mixed genetic architecture where multiple loci, with a
296 variety of effect sizes, control maturation timing – similar to what has been found in male farmed Atlantic
297 salmon [19]. Knowledge of this mixed genetic architecture is highly relevant for how we predict the
298 evolution of maturation timing in wild Atlantic salmon populations. A large body of work has shown the
299 relevance of genetic architecture in determining evolutionary responses [60–68]. Recent works highlight the
300 relevance of the genetic architecture underlying fitness traits when predicting a population’s response to

301 environmental changes [69] and selective pressures such as fishing [70]. Future work elucidating how such
302 mixed genetic architectures affect predicted evolution of traits, compared to that of omnigenic or polygenic
303 architectures, will be valuable.

304 We find differences in locations of top-associated SNPs identified here and in Sinclair-Waters et al.
305 [19]. This is not surprising given that we are examining sequence data that captures more SNP variation
306 compared to SNP-array data used in Sinclair-Waters et al. [19]. Furthermore, we failed to find associations
307 between sea age at maturity and many of the candidate regions identified in Sinclair-Waters et al. [19]. For
308 example, several candidate regions on ssa03 and ssa04 displayed particularly strong association signals in
309 aquaculture salmon, however, no signals at these regions were found here. Additionally, only one association
310 peak at ssa06:27541960-28218141 was found here, whereas two independent associations within this region
311 were found in aquaculture salmon [19]. Such differences may reflect changes in the genetic architecture of
312 the trait evolving since the domestication of Atlantic salmon. Although, we would not expect large changes
313 to occur given the domestication is relatively recent, just 10 to 15 generations ago [71]. Furthermore, this
314 study is likely under-powered to detect all previously identified loci, particularly those with smaller effect
315 sizes or rare alleles, due to smaller sample size. Additionally, there could be differences in genetic
316 architecture among environments [72] and/or genotype by environment interactions giving rise to distinct
317 genetic architectures in wild populations versus aquaculture strains.

318 We do not find strong evidence of multi-SNP associations at candidate loci examined in this study,
319 however, we cannot yet disregard the utility of multi-SNP association methods for further resolving the
320 genetic architecture of Atlantic salmon maturation. First, we do not examine the entire genome due to
321 computational restrictions, rather, we focussed on 116 previously identified candidate regions. Second, the
322 Atlantic salmon genome is highly complex [39] and therefore errors in the assembly that may be disruptive
323 for haplotype-based analysis could exist. As new and improved versions of the Atlantic salmon genome are
324 published, our ability to test for haplotypic associations will improve. Furthermore, in a few cases
325 (ssa09:10915066-11415066, ssa09:24636574-25136574, ssa25:28389273-28889273) the *PiMASS* analyses
326 post-regression of the top SNP selected no SNPs for a model explaining sea age at maturity variation,
327 however, the median proportion of variance explained across all iterations was greater than zero. This may

328 suggest that a weak signal was present, but was being missed due to insufficient power. Although this is
329 largely speculative, it suggests that ruling out the possibility of multi-SNP associations at these particular
330 candidate regions may be premature. Higher-powered studies (i.e. more individuals per population) may help
331 to resolve this in the future.

332 In conclusion, our analytical framework, combining both single and multi-SNP association methods,
333 reveals that single SNP variation is sufficient for explaining the association of previously identified
334 candidate loci for Atlantic salmon maturation timing. Previous empirical and theoretical work have described
335 trait-associated loci that have complex alleles with multiple variants, our findings therefore demonstrate the
336 diversity of genetic architectures for fitness-related traits. Additional data, and a greater diversity of species
337 and traits, will serve to better understand why this diversity of genetic architectures exists and how these
338 particular genetic architectures evolve. The analytical framework used here will be a valuable resource for
339 accomplishing this as individual-level resequencing data for wild species with phenotyped individuals
340 becomes increasingly available.

341

342 **Acknowledgements**

343 Funding was provided by Academy of Finland (grant numbers 307593, 302873 and 327255), the Research
344 Council of Norway (NFR-275310 and NFR-275862) and a Natural Sciences and Engineering Research
345 Council of Canada postgraduate scholarship. Wild Atlantic salmon genome sequencing was funded by the
346 Research Council of Norway (The Aqua Genome project; ref: 221734). We would like to acknowledge
347 Terese Andersstuen, Dr Mariann Árnýasi and Hanna Hellerud Hansen from CIGENE for their work in
348 organising the sequencing of samples. We thank Gunnel Østborg (NINA), Kurt Urdal (Rådgivende Biologer)
349 and Natural Resources Institute Finland (LUKE) for their work collecting phenotype data. We also
350 acknowledge the Aqua Genome project for providing access to data prior to public release. The Orion
351 Computing Cluster at CIGENE-NMBU and CSC – IT Center for Science, Finland are acknowledged for
352 computational resources. Storage resources were provided by the Norwegian National Infrastructure for

353 Research Data (NIRD, project NS9055K). Phenotype data was provided by the Norwegian Institute for
354 Nature Research (NINA).

355 **Data availability**

356 Genome re-sequencing data for individuals used in this study are available in the European Nucleotide
357 Archive (ENA) or NCBI with the project accession code PRJEB38061 [38].

358 **Contributions**

359 CRP, NJB, MSW conceived the study. TN developed the variant calling workflow and constructed the fixed
360 assembly of *ssa25*. JW developed the variant filtering criteria. MSW performed all downstream analyses
361 with input from NJB. MPK played key role in generating whole genome sequencing data. SL led the whole
362 genome sequencing work as part of the AquaGenome project. HS, GHB, BFL, CRP coordinated Atlantic
363 salmon sampling and provided phenotypic information. MSW, CRP, NJB drafted the manuscript. All authors
364 commented on and approved the final manuscript.

365 **Competing interests**

366 There are no competing interests.

367

368 References

- 369 1. Marouli E, Graff M, Medina-Gomez C, Lo KS, Wood AR, Kjaer TR, et al. Rare and low-frequency
370 coding variants alter human adult height. *Nature*. 2017;542(7640):186–90.
- 371 2. Timpson NJ, Greenwood CMT, Soranzo N, Lawson DJ, Richards JB. Genetic architecture: the shape
372 of the genetic contribution to human traits and disease. *Nat Rev Genet*. 2017;
- 373 3. Boyle EA, Li YI, Pritchard JK. An Expanded View of Complex Traits: From Polygenic to
374 Omnigenic. *Cell*. 2017;169(7):1177–86.
- 375 4. Moser G, Lee SH, Hayes BJ, Goddard ME, Wray NR, Visscher PM. Simultaneous Discovery,
376 Estimation and Prediction Analysis of Complex Traits Using a Bayesian Mixture Model. *PLoS*
377 *Genet*. 2015;11(4):1–22.
- 378 5. Loh PR, Bhatia G, Gusev A, Finucane HK, Bulik-Sullivan BK, Pollack SJ, et al. Contrasting genetic
379 architectures of schizophrenia and other complex diseases using fast variance-components analysis.
380 *Nat Genet*. 2015;47(12):1385–92.
- 381 6. Fisher R. The correlations between relatives on the supposition of mendelian inheritance. *Philos*
382 *Trans R Soc Edinburgh*. 1918;52:399–433.
- 383 7. Pritchard JK, Di Rienzo A. Adaptation - not by sweeps alone. *Nat Rev Genet*. 2010;11(10):665–7.
- 384 8. Liu X, Li YI, Pritchard JK. Trans Effects on Gene Expression Can Drive Omnigenic Inheritance.
385 *Cell*. 2019;177(4):1022-1034.e6.
- 386 9. Visscher PM, Wray NR, Zhang Q, Sklar P, McCarthy MI, Brown MA, et al. 10 Years of GWAS
387 Discovery: Biology, Function, and Translation. *Am J Hum Genet* [Internet]. 2017;101(1):5–22.
388 Available from: <http://dx.doi.org/10.1016/j.ajhg.2017.06.005>
- 389 10. Barson NJ, Aykanat T, Hindar K, Baranski M, Bolstad GH, Fiske P, et al. Sex-dependent dominance
390 at a single locus maintains variation in age at maturity in salmon. *Nature*. 2015 Dec
391 17;528(7582):405–8.
- 392 11. Linnen CR, Poh Y-P, Peterson BK, Barrett RDH, Larson JG, Jensen JD, et al. Adaptive evolution of
393 multiple traits through multiple mutations at a single gene. *Science* (80-). 2013;339(6125):1312–6.
- 394 12. Lamichhaney S, Fan G, Widemo F, Gunnarsson U, Thalmann DS, Hoepfner MP, et al. Structural
395 genomic changes underlie alternative reproductive strategies in the ruff (*Philomachus pugnax*). *Nat*
396 *Genet*. 2015;48(1):84–8.
- 397 13. Küpper C, Stocks M, Risse JE, Dos Remedios N, Farrell LL, McRae SB, et al. A supergene
398 determines highly divergent male reproductive morphs in the ruff. *Nat Genet*. 2015;48(1):79–83.
- 399 14. Kirubakaran TG, Grove H, Kent MP, Sandve SR, Baranski M, Nome T, et al. Two adjacent
400 inversions maintain genomic differentiation between migratory and stationary ecotypes of Atlantic
401 cod. *Mol Ecol*. 2016;25:2130–43.
- 402 15. Sinclair-Waters M, Bradbury IR, Morris CJ, Lien S, Kent MP, Bentzen P. Ancient chromosomal
403 rearrangement associated with local adaptation of a post-glacially colonized population of Atlantic
404 Cod in the northwest Atlantic. *Mol Ecol* [Internet]. 2017;(October):1–13. Available from:
405 <http://doi.wiley.com/10.1111/mec.14442>
- 406 16. Pearse DE, Barson NJ, Nome T, Gao G, Campbell MA, Abadía-Cardoso A, et al. Sex-dependent
407 dominance maintains migration supergene in rainbow trout. *bioRxiv* [Internet]. 2018;504621.
408 Available from: <https://www.biorxiv.org/content/early/2018/12/22/504621.article-metrics>
- 409 17. Joron M, Frezal L, Jones RT, Chamberlain NL, Lee SF, Haag CR, et al. polymorphic supergene
410 controlling butterfly mimicry. *Nature*. 2011;

- 411 18. Sinnott-Armstrong N, Naqvi S, Rivas MA, Pritchard JK. GWAS of three molecular traits highlights
412 core genes and pathways alongside a highly polygenic background. *bioRxiv*.
413 2020;2020.04.20.051631.
- 414 19. Sinclair-Waters M, Ødegård J, Korsvoll SA, Moen T, Lien S, Primmer CR, et al. Beyond large-effect
415 loci: large-scale GWAS reveals a mixed large-effect and polygenic architecture for age at maturity of
416 Atlantic salmon. *Genet Sel Evol* [Internet]. 2020;52(1):9. Available from:
417 <https://doi.org/10.1186/s12711-020-0529-8>
- 418 20. Bickel RD, Kopp A, Nuzhdin S V. Composite effects of polymorphisms near multiple regulatory
419 elements create a major-effect QTL. *PLoS Genet*. 2011;7(1):1–8.
- 420 21. Kerdaffrec E, Filiault DL, Korte A, Sasaki E, Nizhynska V, Seren Ü, et al. Multiple alleles at a single
421 locus control seed dormancy in Swedish Arabidopsis. *Elife* [Internet]. 2016 Dec 14;5(3):1–24.
422 Available from: <http://elifesciences.org/lookup/doi/10.7554/eLife.22502>
- 423 22. Yeaman S, Whitlock MC. The genetic architecture of adaptation under migration-selection balance.
424 *Evolution* (N Y). 2011;65(7):1897–911.
- 425 23. Yeaman S. Genomic rearrangements and the evolution of clusters of locally adaptive loci. *Proc Natl*
426 *Acad Sci U S A* [Internet]. 2013;110:E1743-51. Available from:
427 [http://www.pubmedcentral.nih.gov/articlerender.fcgi?artid=3651494&tool=pmcentrez&rendertype=a](http://www.pubmedcentral.nih.gov/articlerender.fcgi?artid=3651494&tool=pmcentrez&rendertype=abstract)
428 [b](http://www.pubmedcentral.nih.gov/articlerender.fcgi?artid=3651494&tool=pmcentrez&rendertype=abstract)stract
- 429 24. Remington DL. Alleles versus mutations: Understanding the evolution of genetic architecture
430 requires a molecular perspective on allelic origins. *Evolution* (N Y). 2015;69(12):3025–38.
- 431 25. Stearns SC. Life history evolution: Successes, limitations, and prospects. *Naturwissenschaften*.
432 2000;87(11):476–86.
- 433 26. Mobley KB, Aykanat T, Czorlich Y, House A, Kurko J, Miettinen A, et al. Maturation in Atlantic
434 salmon (*Salmo salar*, Salmonidae): a review of ecological, genetic, and molecular processes. *FEBS*
435 *Lett*. 2020;(November):1–58.
- 436 27. Fleming IA, Einum S. Reproductive ecology: a tale of two sexes. In: *Atlantic Salmon Ecology*. 2011.
437 p. 35–65.
- 438 28. Mobley KB, Granroth-Wilding H, Ellmén M, Orell P, Erkinaro J, Primmer CR. Time spent in distinct
439 life history stages has sex-specific effects on reproductive fitness in wild Atlantic salmon. *Mol Ecol*.
440 2020;29(6):1173–84.
- 441 29. Gjerde B. Response to individual selection for age at sexual maturity in Atlantic salmon.
442 *Aquaculture*. 1984;38(3):229–40.
- 443 30. Reed TE, Prodöhl PA, Bradley C, Gilbey J, McGinnity P, Primmer CR, et al. Heritability estimation
444 via molecular pedigree reconstruction in a wild fish population reveals substantial evolutionary
445 potential for sea-age at maturity, but not size within age-classes. *Can J Fish Aquat Sci* [Internet].
446 2018;cjfas-2018-0123. Available from: [http://www.nrcresearchpress.com/doi/10.1139/cjfas-2018-](http://www.nrcresearchpress.com/doi/10.1139/cjfas-2018-0123)
447 [0123](http://www.nrcresearchpress.com/doi/10.1139/cjfas-2018-0123)
- 448 31. Ayllon F, Kjærner-Semb E, Furmanek T, Wennevik V, Solberg MF, Dahle G, et al. The *vgl13* Locus
449 Controls Age at Maturity in Wild and Domesticated Atlantic Salmon (*Salmo salar* L.) Males. *PLoS*
450 *Genet*. 2015;11(11):1–15.
- 451 32. Sinclair-Waters M, Piavchenko N, Ruokolainen A, Aykanat T, Erkinaro J, Primmer CR. Refining the
452 genomic location of SNP variation affecting Atlantic salmon maturation timing at a key large-effect
453 locus. *bioRxiv* [Internet]. 2021; Available from:
454 <https://www.biorxiv.org/content/early/2021/04/26/2021.04.26.441431>
- 455 33. Halperin DS, Pan C, Lusic AJ, Tontonoz P. Vestigial-like 3 is an inhibitor of adipocyte

- 456 differentiation. *J Lipid Res.* 2013;54(2):473–81.
- 457 34. Day FR, Thompson DJ, Helgason H, Chasman DI, Finucane H, Sulem P, et al. Genomic analyses
458 identify hundreds of variants associated with age at menarche and support a role for puberty timing in
459 cancer risk. *Nat Genet.* 2017;49(6):834–41.
- 460 35. Perry JRB, Day F, Elks CE, Sulem P, Thompson DJ, Ferreira T, et al. Parent-of-origin-specific allelic
461 associations among 106 genomic loci for age at menarche. *Nature.* 2014 Jul 23;514:92.
- 462 36. Waters CD, Clemento A, Aykanat T, Garza JC, Naish KA, Narum S, et al. Heterogeneous genetic
463 basis of age at maturity in salmonid fishes. *Molecular Ecol.* 2021;
- 464 37. Cánovas A, Reverter A, DeAtley KL, Ashley RL, Colgrave ML, Fortes MRS, et al. Multi-tissue
465 omics analyses reveal molecular regulatory networks for puberty in composite beef cattle. *PLoS One.*
466 2014;9(7):1–17.
- 467 38. Bertolotti AC, Layer RM, Gundappa MK, Gallagher MD, Pehlivanoglu E, Nome T, et al. The
468 structural variation landscape in 492 Atlantic salmon genomes. *Nat Commun [Internet].*
469 2020;11(5176). Available from: <https://doi.org/10.1101/2020.05.16.099614>
- 470 39. Lien S, Koop BF, Sandve SR, Miller JR, Kent MP, Nome T, et al. The Atlantic salmon genome
471 provides insights into rediploidization. *Nature.* 2016 May 12;533(7602):200–5.
- 472 40. Chapman B, Kirchner R, Pantano L, Smet M De, Beltrame L, Khotiainsteva T, et al. bcbio/bcbio-
473 nextgen: v1.2.3. 2020 Apr 7 [cited 2020 Sep 17]; Available from: <https://zenodo.org/record/3743344>
- 474 41. Li H. Aligning sequence reads, clone sequences and assembly contigs with BWA-MEM. *arXiv*
475 [Internet]. 2013 Mar 16 [cited 2020 Sep 17]; Available from: <https://arxiv.org/abs/1303.3997>
- 476 42. Picard toolkit. Broad Institute, GitHub repository. Broad Institute; 2019.
- 477 43. DePristo MA, Banks E, Poplin R, Garimella K V., Maguire JR, Hartl C, et al. A framework for
478 variation discovery and genotyping using next-generation DNA sequencing data. *Nat Genet.*
479 2011;43(5):491–501.
- 480 44. Cingolani P, Platts A, Wang LL, Coon M, Nguyen T, Wang L, et al. A program for annotating and
481 predicting the effects of single nucleotide polymorphisms, SnpEff: SNPs in the genome of *Drosophila*
482 *melanogaster* strain w1118; iso-2; iso-3. *Fly (Austin).* 2012;6(2):80–92.
- 483 45. Li H. SNPable Regions [Internet]. 2009. Available from:
484 <http://lh3lh3.users.sourceforge.net/snpable.shtml>
- 485 46. Li H, Durbin R. Fast and accurate short read alignment with Burrows-Wheeler transform.
486 *Bioinformatics.* 2009 Jul;25(14):1754–60.
- 487 47. Danecek P, Auton A, Abecasis G, Albers C, Banks E, DePristo M. The variant call format and
488 vcfTools. *Bioinformatics.* 2011;27(15):2156–2158.
- 489 48. Purcell S, Neale B, Todd-Brown K, Thomas L, Ferreira M, Bender D. Plink: A tool set for whole-
490 genome association and population-based linkage analyses. *Am J Hum Genet [Internet].* 2007;81.
491 Available from: <https://doi.org/10.1086/519795>
- 492 49. Patterson N, Price AL, Reich D. Population Structure and Eigenanalysis. *PLoS Genet.* 2006;2(12).
- 493 50. Quinlan AR, Hall IM. BEDTools: A flexible suite of utilities for comparing genomic features.
494 *Bioinformatics.* 2010;26(6):841–2.
- 495 51. Camacho C, Coulouris G, Avagyan V, Ma N, Papadopoulos J, Bealer K, et al. BLAST+: Architecture
496 and applications. *BMC Bioinformatics.* 2009;10:1–9.
- 497 52. Xu H, Guan Y. Detecting local haplotype sharing and haplotype association. *Genetics.*
498 2014;197(3):823–38.

- 499 53. Guan Y. Detecting structure of haplotypes and local ancestry. *Genetics*. 2014;196(3):625–42.
- 500 54. Chang CC, Chow CC, Tellier LCAM, Vattikuti S, Purcell SM, Lee JJ. Second-generation PLINK:
501 rising to the challenge of larger and richer datasets. *Gigascience*. 2015 Feb;4(1):7.
- 502 55. Guan Y, Stephens M. Bayesian variable selection regression for genome-wide association studies and
503 other large-scale problems. *Ann Appl Stat*. 2011;5(3):1780–815.
- 504 56. Harold Jeffreys. *The Theory of Probability*. 2020. 470 p.
- 505 57. Allendorf FW, Thorgaard GH. *Tetraploidy and the Evolution of the Salmonid Fishes*. Springer.
506 *Monographs in Evolutionary Biology*. Boston; 1984. 55–93 p.
- 507 58. Yeaman S, Aeschbacher S, Bürger R. The evolution of genomic islands by increased establishment
508 probability of linked alleles. *Mol Ecol [Internet]*. 2016 Jun 1;25(11):2542–58. Available from:
509 <https://doi.org/10.1111/mec.13611>
- 510 59. Ayllon F, Solberg MF, Glover KA, Mohammadi F, Kjærner-semb E, Fjellidal PG, et al. The influence
511 of *vgl13* genotypes on sea age at maturity is altered in farmed mowi strain Atlantic salmon. *BMC*
512 *Genet*. 2019;20(44):1–8.
- 513 60. Barton NH, Turelli M. Natural and sexual selection on many loci. *Genetics*. 1991 Jan;127(1):229–55.
- 514 61. Turelli M. Heritable genetic variation via mutation-selection balance: Lerch’s zeta meets the
515 abdominal bristle. *Theor Popul Biol*. 1984 Apr;25(2):138–93.
- 516 62. Turelli M, Barton NH. Polygenic Variation Maintained by Balancing Selection: Pleiotropy, Sex-
517 Dependent Allelic Effects and $G \times E$ Interactions. *Genetics*. 2004;166(2):1053–79.
- 518 63. Turelli M, Barton NH. Dynamics of polygenic characters under selection. *Theor Popul Biol*.
519 1990;38(1):1–57.
- 520 64. Lande R. The maintenance of genetic variability by mutation in a polygenic character with linked
521 loci. *Genet Res*. 2009/04/14. 1975;26(3):221–35.
- 522 65. Bulmer MG. The genetic variability of polygenic characters under optimizing selection, mutation and
523 drift. *Genet Res (Camb)*. 1972;19(1):17–25.
- 524 66. Débarre F, Yeaman S, Guillaume F. Evolution of Quantitative Traits under a Migration-Selection
525 Balance : When Does Skew Matter ?*. *Am Nat*. 2015;186.
- 526 67. Fisher R. *The genetical theory of natural selection*. Clarendon, Oxford; 1930.
- 527 68. Yeaman S. Local Adaptation by Alleles of Small Effect *. *Am Nat*. 2015;186.
- 528 69. Kardos M, Luikart G. The genetic architecture of fitness drives population viability during rapid
529 environmental change. *Am Nat*. 2021;
- 530 70. Oomen RA, Kuperinen A, Hutchings JA. Consequences of Single-Locus and Tightly Linked
531 Genomic Architectures for Evolutionary Responses to Environmental Change. *J Hered [Internet]*.
532 2020;319–32. Available from: <https://academic.oup.com/jhered/article/111/4/319/5867197>
- 533 71. Gjerde B, Gjedrem T. Estimates of phenotypic and genetic parameters for carcass traits in Atlantic
534 salmon and rainbow trout. *Aquaculture*. 1984;36(1–2):97–110.
- 535 72. Yan W, Wang B, Chan E, Mitchell-Olds T. Genetic architecture and adaptation of flowering time
536 among environments. *New Phytol [Internet]*. 2021 Jan 23;n/a(n/a). Available from:
537 <https://doi.org/10.1111/nph.17229>

538